

# Oridonin inhibits VEGF-A-associated angiogenesis and epithelial-mesenchymal transition of breast cancer *in vitro* and *in vivo*

CHUNYU LI<sup>1</sup>, QI WANG<sup>2</sup>, SHEN SHEN<sup>1</sup>, XIAOLU WEI<sup>1</sup> and GUOXIA LI<sup>1</sup>

<sup>1</sup>Department of Integrated Chinese Traditional and Western Medicine, International Medical School, Tianjin Medical University, Tianjin 300070; <sup>2</sup>Department of Oncology, Shanghai Pulmonary Hospital Affiliated to Tongji University, Shanghai 200433, P.R. China

Received November 10, 2017; Accepted June 6, 2018

DOI: 10.3892/ol.2018.8943

**Abstract.** Metastasis is the primary cause of mortality in patients with breast cancer and lacks effective therapeutic agents. Oridonin, an active diterpenoid compound isolated from *Rabdosia rubescens*, was identified to be the most potent anti-tumor ingredient. However, the molecular mechanisms responsible for its anti-metastatic effects remain unclear. In the present study, oridonin significantly suppressed the migration, invasion and adhesion of MDA-MB-231 and 4T1 breast cancer cells, and inhibited tube formation of human umbilical vein endothelial cells in a dose-dependent manner. The expression levels of epithelial-mesenchymal transition (EMT)-associated marker and the hypoxia inducible factor 1 $\alpha$  (HIF-1 $\alpha$ )/vascular endothelium growth factor (VEGF) signaling pathway mRNA and proteins were determined by reverse transcription-quantitative polymerase chain reaction and western blotting, respectively *in vitro*. The results demonstrated that oridonin effectively inhibited EMT as demonstrated by the significant increases in the expression levels of E-cadherin, and decreased expression of N-cadherin, Vimentin and Snail. In addition, oridonin exerted its anti-angiogenesis activity through significantly decreasing HIF-1 $\alpha$ , VEGF-A and VEGF receptor-2 protein expression. Furthermore, oridonin was demonstrated to decrease the micro-vessel density as evidenced by the decreased expression of cluster of differentiation 31, a marker for neovasculature. In brief, oridonin inhibits tumor cell migration, invasion and adhesion, as well as tumor angiogenesis, which are mediated by suppressing EMT and the HIF-1 $\alpha$ /VEGF signaling pathway.

The results of the present study suggest that oridonin may be a promising anti-metastatic agent in breast cancer treatment.

## Introduction

Breast cancer is the most fatal type of malignancy and the second leading cause of cancer-associated mortalities among women worldwide (1). Approximately 90% of breast cancer-associated mortalities are due to metastasis to distant sites and not by the primary tumor itself. Therefore, screening for more effective compounds to control breast cancer metastasis has become the most important factor in improving breast cancer treatment.

During cancer progression, epithelial-mesenchymal transition (EMT) process is one of the primary mechanisms involved in breast cancer metastasis (2). The process of EMT, during which cells lose epithelial characteristics and obtain mesenchymal properties, promotes cancer cell metastasis from primary tumors (3). In addition to EMT, angiogenesis is another important factor that promotes tumor growth metastasis (4). Accumulating evidence suggests that vascular endothelium growth factor (VEGF) is an essential factor in the development of tumor angiogenesis (5). Hypoxia inducible factor 1 $\alpha$  (HIF-1 $\alpha$ ), upstream of the VEGF, is associated with poor prognosis, and an increased risk of metastasis and mortality (6). Hypoxia, a common characteristic of solid tumors, has been reported to reactivate EMT through HIF-1 $\alpha$  in several tumor models (7). HIF-1 $\alpha$  directly or indirectly regulates EMT regulators, including Snail, Twist1 and Slug, and other transcription factors, and these transcription factors then trans activate EMT-associated genes, including E-cadherin, Vimentin and N-cadherin, to mediate EMT (8). Accordingly, EMT and angiogenesis have become therapeutic targets for cancer metastasis treatment.

Oridonin, an active diterpenoid compound isolated from *Rabdosia rubescens*, is currently one of the most important active Chinese medicinal components. Notably, several studies reported that oridonin also demonstrates significant anti-metastasis effect in a variety of cancer types (9). For instance, Dong *et al* (10) confirmed that oridonin inhibits tumor growth and metastasis through anti-angiogenesis by

---

*Correspondence to:* Dr Chunyu Li, Department of Integrated Chinese Traditional and Western Medicine, International Medical School, Tianjin Medical University, 22 Qixiangtai Road, Heping, Tianjin 300070, P.R. China  
E-mail: lichunyu@tmu.edu.cn

**Key words:** oridonin, epithelial-mesenchymal transition, angiogenesis, metastasis, breast cancer

blocking the Notch signaling. Liu *et al* (11) indicated that the oridonin anti-tumor effect was primarily based on its anti-proliferation and anti-angiogenesis properties. Although accumulating evidence have indicated the anti-metastatic potential of oridonin, the effects and underlying mechanisms of oridonin on human breast cancer cells have not been fully elucidated. The present study investigated the effects of oridonin on EMT and angiogenesis in breast cancer, and its underlying mechanisms.

## Materials and methods

**Animals.** A total of 24 female BALB/c mice (5-6 weeks old, 14-16 g) were purchased from the Laboratory Animal Center of the Academy of Military Medical Sciences (Beijing, China) and housed in a temperature-controlled vivarium on a 12/12 h light/dark cycle. Standard rodent diet and water were provided *ad libitum* except where noted. All animal experiments were approved by the Animal Ethics Committee of Tianjin Medical University (Tianjin, China) and complied with its regulations.

**Reagents and antibodies.** Oridonin (CAS no. 28957-04-2) was acquired from Aladdin Shanghai Biochemical Technology Co., Ltd. (Shanghai, China). MTT, dimethyl sulfoxide (DMSO) and albumin fraction V (BSA) were purchased from Sigma-Aldrich (Merck KGaA, Darmstadt, Germany). Dulbecco's modified Eagle's medium (DMEM), fetal bovine serum (FBS) and penicillin/streptomycin were purchased from Gibco (Thermo Fisher Scientific Inc., Waltham, MA, USA). Antibodies against E-cadherin (mouse; cat. no. 14472), N-cadherin (rabbit; cat. no. 13116), Vimentin (mouse; cat. no. 3390) and Snail (mouse; cat. no. 3895) were purchased from Cell Signaling Technology, Inc. (Danvers, MA, USA). Antibodies against HIF-1 $\alpha$  (mouse; cat. no. ab113642), VEGF-A (rabbit; cat. no. ab46154), VEGFR-2 (rabbit; cat. no. ab2349),  $\beta$ -actin (rabbit; cat. no. ab8227) and CD31 (rabbit; cat. no. ab32457) were purchased from Abcam (Cambridge, MA, USA). Goat anti-mouse IgG-horseradish peroxidase (HRP) (cat. no. sc-2005) and goat anti-rabbit IgG-HRP (cat. no. sc-2004) were purchased from Santa Cruz Biotechnology, Inc. (Dallas, TX, USA).

**Cell culture.** Human breast cancer cells MDA-MB-231, non-tumorigenic human breast cells MCF-10A and human umbilical vein epithelial cells (HUVECs; cat. no. PCS-100-013) were obtained from the American Type Culture Collection (Manassas, VA, USA). Mouse breast cancer cells 4T1 were purchased from the Type Culture Collection of the Chinese Academy of Sciences (Shanghai, China). The cells were cultured in DMEM supplemented with 10% FBS, 100 U/ml penicillin and 100  $\mu$ g/ml streptomycin. Hypoxia was induced by exposing the cells to 150  $\mu$ M CoCl<sub>2</sub> (Sigma-Aldrich; Merck KGaA) in DMEM with 0.5% FBS for 24 h (12). All cell cultures were maintained at 37°C in an atmosphere containing 5% CO<sub>2</sub>.

**MTT assay.** Cell viability was measured using an MTT assay. The MDA-MB-231, MCF-10A and 4T1 cells in the logarithm phase were seeded in 96-well culture plates at the density of 5x10<sup>3</sup> cells/well. When the cells were adherent to the walls,

the cells were treated with oridonin (2, 4, 8, 16, 32 and 64  $\mu$ M) for 48 h followed by the addition of 100  $\mu$ l MTT (1 mg/ml) and incubation for 4 h. Then, the medium was removed and 150  $\mu$ l of DMSO was added to each well. Absorbance of each well was detected at 490 nm using microplate reader. The experiment was repeated three times. The inhibition rate (% of control) was calculated as follows: [1-(absorbance of test sample/absorbance of control)] x100%.

**Wound healing migration assay.** Cell migration was detected using a wound-healing assay. MDA-MB-231 and 4T1 cells were cultured in 60-mm dishes at the density of 8x10<sup>5</sup> cells/dish to 100% confluence. Following wounding with a pipette tip, the cells were washed with PBS and serum-free medium with 4, 8 or 16  $\mu$ M oridonin. Then, the cells were allowed to migrate for 24 h at 37°C in 5% CO<sub>2</sub>. At predetermined time points (0, 3, 6, 9, 12 and 24 h), the widths of wound were measured using a ruler, and images of the cells were captured at 0 and 24 h under a light microscope with x100 magnification (IX71; Olympus Corporation, Tokyo, Japan).

**Transwell invasion assay.** Cell invasion was detected using a Transwell assay. Following pre-treatment with 4, 8 or 16  $\mu$ M oridonin for 24 h, MDA-MB-231 and 4T1 cells were harvested and seeded in the upper chamber of the Transwell chamber coated with Matrigel (BD Biosciences, San Jose, CA, USA) at a density of 4x10<sup>4</sup> cells/well in serum-free medium. The lower chambers were filled with standard medium. The cells were allowed to invade for 24 h incubated at 37°C in 5% CO<sub>2</sub>. The invading cells were fixed with 4% methanol for 20 min at room temperature. Cell numbers were counted in five separate fields using a computer-based microcopy imaging DP2-BSW system (version 1.3; Olympus Corporation).

**Cell adhesion assay.** Following pre-treatment with 4, 8 or 16  $\mu$ M oridonin for 24 h, MDA-MB-231 and 4T1 cells were harvested, re-suspended in serum free medium at the density of 2x10<sup>5</sup> cells/well and seeded to the 24-well plates coated with fibronectin (10 ng/ml). Following further incubations for 5, 15 and 30 min, non-adherent cells were removed by three PBS washes. The adherent cells were fixed with 4% methanol for 20 min at room temperature and counted in five separate fields under a light microscope with x200 magnification (Olympus Corporation).

**Tube formation assay.** AHUVEC capillary-like formation assay was performed on Matrigel (BD Biosciences) (13). Matrigel was added into 96-well plate and cultured in 37°C for 2 h to solidify the Matrigel. Following pre-treatment with 4, 8 or 16  $\mu$ M oridonin for 24 h, HUVECs were seeded in plates at the density of 8x10<sup>3</sup> cells/well. According to previous methods (14,15), morphological changes (formation of capillary-like structures) of the cells and tube formation were observed under a phase-contrast microscope and imaged at x200 magnification after a 6 h incubation.

**Reverse transcription-quantitative polymerase chain reaction (RT-qPCR).** Following pre-treatment with 4, 8 or 16  $\mu$ M oridonin for 24 h, the total RNA of MDA-MB-231 or 4T1 cells was extracted using TRIzol reagent (Life Technologies;

Thermo Fisher Scientific, Inc.). Reverse transcription was performed with the fast quant RT kit (Tiangen Biotech Co., Ltd., Beijing, China) according to the manufacturer's protocol. The PCR mixture volume was 25  $\mu$ l, including 12.5  $\mu$ l SYBR green mix (Tiangen Biotech Co., Ltd.), 0.2  $\mu$ l cDNA, 1.5  $\mu$ l primer/mix (10  $\mu$ M of each primer) and 10.8  $\mu$ l RNase-free H<sub>2</sub>O. The experiment was then set up using the following PCR program on a ABI 7500 system (Applied Biosystems; Thermo Fisher Scientific, Inc.): 95°C for 15 min, 1 cycle; followed by 40 cycles of 95°C for 10 sec, 60°C for 20 sec and 72°C for 30 sec. Specific primers were designed using Gene Runner software (version 6.5.48) produced by Dr. Spruyt Michael (Mahwah, NJ, USA) and Dr. Buquicchio Frank (Old Tappan, NJ, USA). Specific primers were synthesized by Beijing Century Aoke Biotechnology Co., Ltd. (Beijing, China). The specific primers are presented in Table I. The Cq value was automatically calculated by 7500 software (version 2.0.5, Applied Biosystems; Thermo Fisher Scientific, Inc.), the Ct values were all normalized against the quantity of the  $\beta$ -actin control RNA, and the relative quantification of gene expression was calculated by the  $2^{-\Delta\Delta Cq}$  method according to the formula:  $\Delta Cq$  (target gene) = Cq (target gene) - Cq (control gene) (16). All assays were performed in triplicate and independently repeated three times.

**Western blotting assay.** Western blotting assay was used for the detection of E-cadherin, N-cadherin, Vimentin, Snail, HIF-1 $\alpha$ , VEGF-A and VEGFR-2 expression levels in MDA-MB-231 and 4T1 cells. Following pre-treatment with 4, 8 or 16  $\mu$ M oridonin for 24 h, the 10  $\mu$ g protein lysates from cultured cells were separated by 10% SDS-PAGE systems and transferred to polyvinylidene difluoride membranes (EMD Millipore, Billerica, MA, USA). Following blocking with 5% skim milk in TBS containing 0.1% Tween 20 (TBST) for 2 h at room temperature, the membranes were incubated with the aforementioned primary antibodies at 1:500 to 1:1,000 dilutions with 5% BSA in TBST overnight at 4°C. The antibodies and dilution factors were as follows: E-cadherin (1:1,000); N-cadherin (1:1,000); Vimentin (1:1,000); Snail (1:1,000); HIF-1 $\alpha$  (1:500); VEGF-A (1:800); and VEGFR-2 (1:800). The blots were washed with PBS and incubated with HRP-conjugated secondary antibodies for 1 h at room temperature. Membranes were visualized using enhanced chemiluminescence kit (EMD Millipore) and were imaged using G-BOX (Gene Company, Ltd., Hong Kong, China). The bands analyzed using Image Pro Plus 6.0 software (Media Cybernetics Inc., Rockville, MD, USA).

**Animal experiments.** The 4T1 (3x10<sup>6</sup>) cells were subcutaneously inoculated into the mammary fat pad of mice. Once each animal developed distinct tumors, animals were randomly segregated into 1 vehicle group and 3 oridonin group (n=6/group) and respectively treated with 0.5% DMSO (the vehicle) or oridonin at doses of 2.5, 5 or 10 mg/kg. All administrations were carried out via intratumoral injections every 3 days four times. Bodyweight and tumor volumes were measured twice a week. The tumor volume was estimated using the following formula: (ab)<sup>2</sup>/2, where a and b are tumor length and width, respectively (17). The animals were sacrificed on day 10, and the tumors of the oridonin-treated and vehicle-treated groups were excised.

Table I. Primers sequences used in RT-qPCR.

Gene name	Primer sequence (5'-3')
E-cadherin	
F	GGATTGCAAATTCCTGCCATTC
R	AACGTTGTCCCGGGTGTCA
Vimentin	
F	GCAGGAGGCAGAAGAATGGTA
R	GGGACTCATTGGTTCCTTAAAGG
Snail	
F	TCTAGGCCCTGGCTGCTACAA
R	CATCTGAGTGGGTCTGGAGGTG
N-cadherin	
F	GAGAGGAAGACCAGGACTATGA
R	CAGTCATCACCACCACCATAC
$\beta$ -actin	
F	CCACGAAACTACCTTCAACTCCA
R	GTGATCTCCTTCTGCATCCTGTC

F, forward; R, reverse; RT-qPCR, reverse transcription-quantitative polymerase chain reaction.

**Immunohistochemical analysis.** Immunohistochemical analysis was performed to evaluate the tumor vessels density. Tumor tissues were fixed in 8% neutral formaldehyde at room temperature, embedded in paraffin and cut into sections of 5-mm thickness. Following antigen retrieval, tissue sections were blocked with PBS containing blocking serum (Gibco; Thermo Fisher Scientific, Inc.) for 2 h at room temperature and were incubated overnight at 4°C with primary antibodies against CD31 at 1:500 dilutions with 5% BSA in TBST (cat. no. AR0195; Boster, Wuhan, China). Subsequently, sections were incubated with universal HRP-conjugated secondary antibodies (OriGene Technologies, Inc., Beijing, China) for 30 min. The chromogenic reaction was performed using DAB peroxidase substrate (OriGene Technologies, Inc.) by incubating sections for 2 min at room temperature. Images were captured with an upright fluorescent microscope (BX51; Olympus Corporation). The number of CD31-positive vessels (brown staining) in five randomly selected fields (magnification, x200) was counted and vessels were calculated as the sum of CD31-positive vessels in the five fields (18).

**Statistical analysis.** Statistical analysis was performed using SPSS 19.0 (IBM Corp., Armonk, NY, USA). All data are presented as the mean  $\pm$  standard deviation. One-way analysis of variance was used to analyze the difference between the groups. The least significant difference method was used to analyze post-hoc multiple comparisons. P-values were two-tailed; P<0.05 was considered to indicate a statistically significant difference.

## Results

**Effects of oridonin on the viability of MDA-MB-231, 4T1 and MCF-10A cells.** Oridonin has a molecular weight of

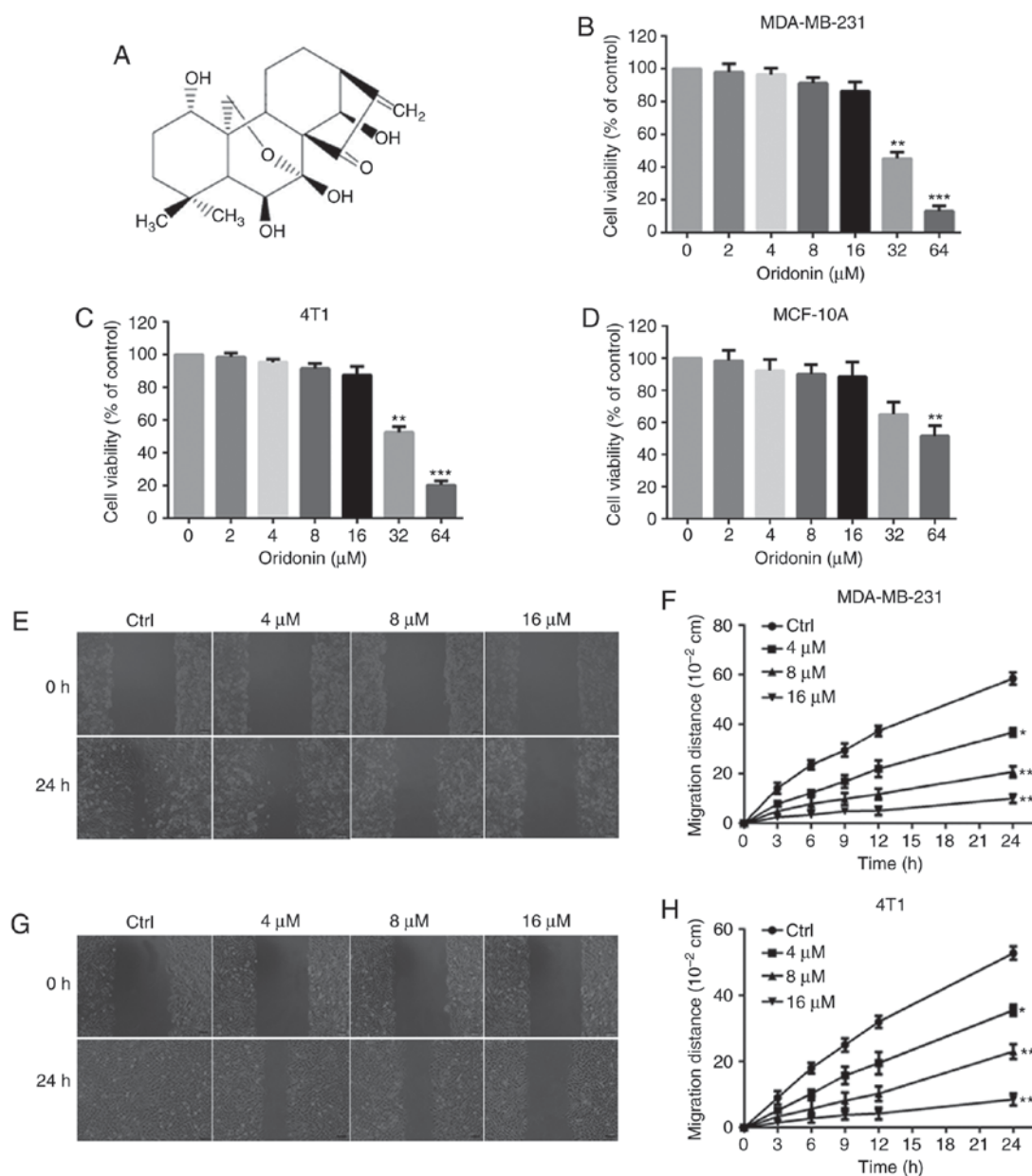


Figure 1. Effects of oridonin on the viability and migratory ability of breast cancer or non-tumorigenic human breast cells. (A) Chemical structure of oridonin. (B) MDA-MB-231, (C) 4T1, and (D) MCF-10A cells were treated with indicated concentrations of oridonin for 48 h and then cell viability was quantified by MTT assay. (E and F) MDA-MB-231 and (G and H) 4T1 cells were treated with the indicated concentrations of oridonin for 24 h. Images were captured at 0 and 24 h after the wound was made. The migration distance was measured using a microscope. Data are presented as the mean  $\pm$  standard deviation of three independent experiments. \* $P < 0.05$ , \*\* $P < 0.01$  and \*\*\* $P < 0.001$  compared with the control group. Ctrl, control.

364.44 g/mol and its molecular structure is presented in Fig. 1A. Firstly, the inhibitory effects of oridonin on the proliferation of MDA-MB-231 and 4T1 cells were investigated using an MTT assay. The results demonstrated that oridonin treatment caused significant cell proliferation inhibition in a dose-dependent manner in MDA-MB-231 and 4T1 cells (Fig. 1B and C). The  $\text{IC}_{50}$  value of oridonin after 48 h of incubation was 29.33 and 33.78  $\mu\text{M}$  for MDA-MB-231 and 4T1 cells, respectively. No significant differences were observed in the viability of MDA-MB-231 and 4T1 cells following exposure to oridonin (4, 8 and 16  $\mu\text{M}$ ) for 48 h. Oridonin at 4, 8 and 16  $\mu\text{M}$  alone exhibited no significant anti-proliferative and cytotoxic effects in non-tumorigenic human breast cells MCF-10A ( $\text{IC}_{50}$  value, 67.94  $\mu\text{M}$ ) (Fig. 1D).

Thus, in the subsequent experiments, the concentrations 4, 8 and 16  $\mu\text{M}$  oridonin were chosen for further investigation. For all *in vitro* experiments, an untreated group was used as the control.

*Oridonin inhibits the migration and invasion of MDA-MB-231 and 4T1 cells.* In the absence of oridonin (control group), MDA-MB-231 and 4T1 cells exhibited high migratory and invasive capabilities as indicated through the complete healing of the wound scratch and penetration of cells through the Matrigel-coated filters. The migration (Fig. 1E-H) and invasion (Fig. 2A-C) of cancer cells was significantly suppressed by oridonin in a concentration-dependent manner.

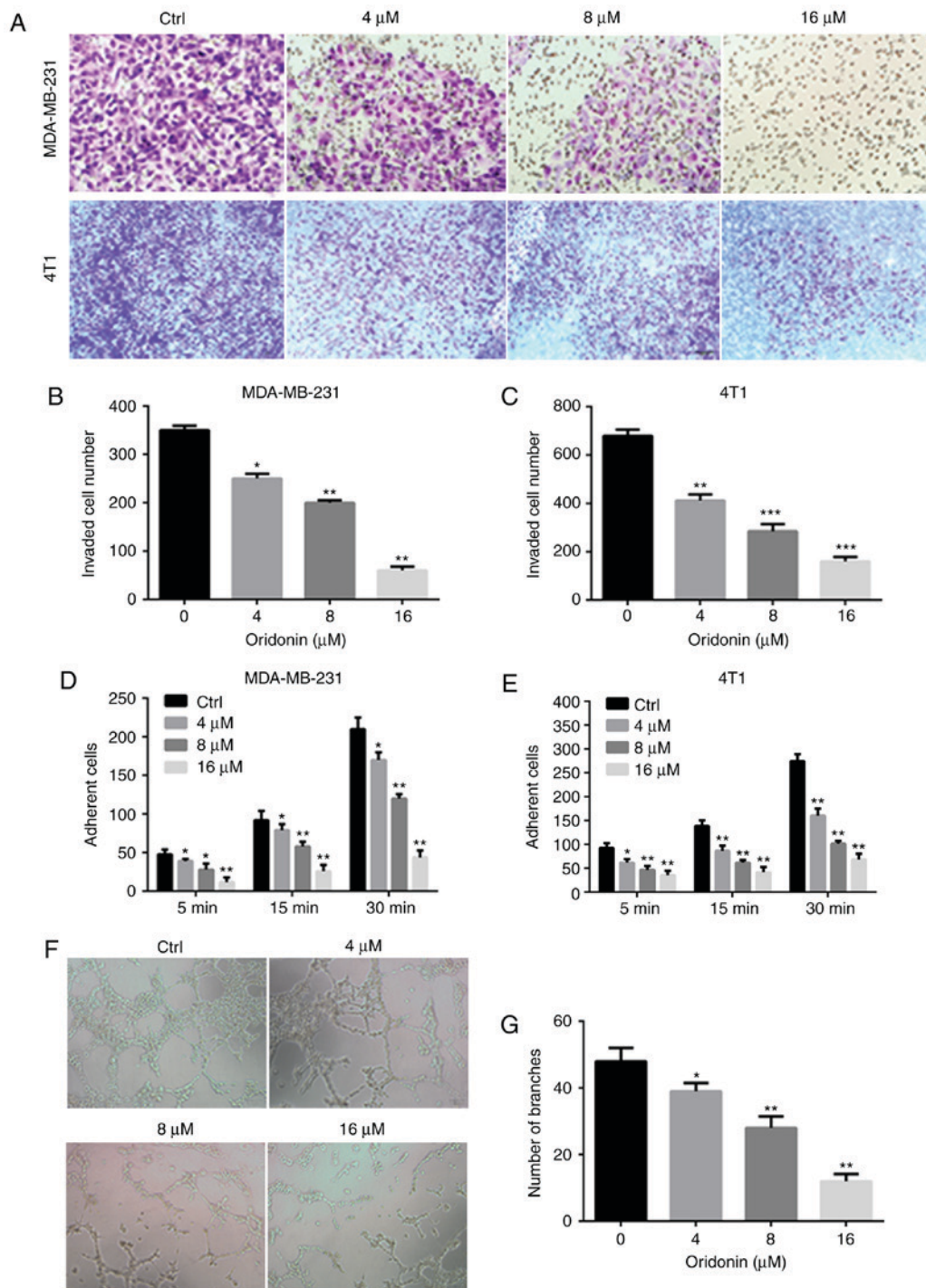


Figure 2. Effects of oridonin on the invasion and adhesion ability of breast cancer cells and angiogenesis of HUVECs. (A) MDA-MB-231 and 4T1 cells were treated with indicated concentrations of oridonin for 24 h and the number of invasive cells was determined using a Transwell invasion assay (magnification,  $\times 200$ ). (B) MDA-MB-231 and (C) 4T1 cells which invaded were fixed with methanol and stained with Giemsa. Cell numbers were counted in five separated fields using the computer-based microscopy imaging system. (D) MDA-MB-231 and (E) 4T1 cells were pre-treated with indicated concentrations of oridonin for 24 h, followed by measuring adhesion capacity on fibronectin over indicated time periods. Cell numbers in five fields were counted for each slide under the microscope. Human umbilical vein epithelial cells were pre-treated with indicated concentrations of oridonin for 24 h. Capillary tube formation was assessed after 6 h. (F) Images were captured and the total number of nodes and (G) branches were calculated under a phase-contrast microscope (magnification,  $\times 200$ ). Data are presented as the mean  $\pm$  standard deviation of three independent experiments. \* $P < 0.05$ , \*\* $P < 0.01$  and \*\*\* $P < 0.001$  compared with the control group. Ctrl, control.

*Oridonin inhibits the adhesion of MDA-MB-231 and 4T1 cells.* Fibronectin was used as the basement membrane to mimic the adhesion of MDA-MB-231 and 4T1 cells (19). Following pre-treatment with 4, 8 and 16  $\mu\text{M}$  oridonin, the number of cells adhering to the fibronectin significantly decreased compared with the control group (Fig. 2D and E).

The results demonstrated that oridonin inhibited the adhesion of MDA-MB-231 and 4T1 cells to fibronectin.

*Oridonin inhibits tube formation of HUVECs cells in vitro.* To investigate the effect of oridonin on angiogenesis *in vitro*, a capillary tube formation assay using HUVECs on Matrigel

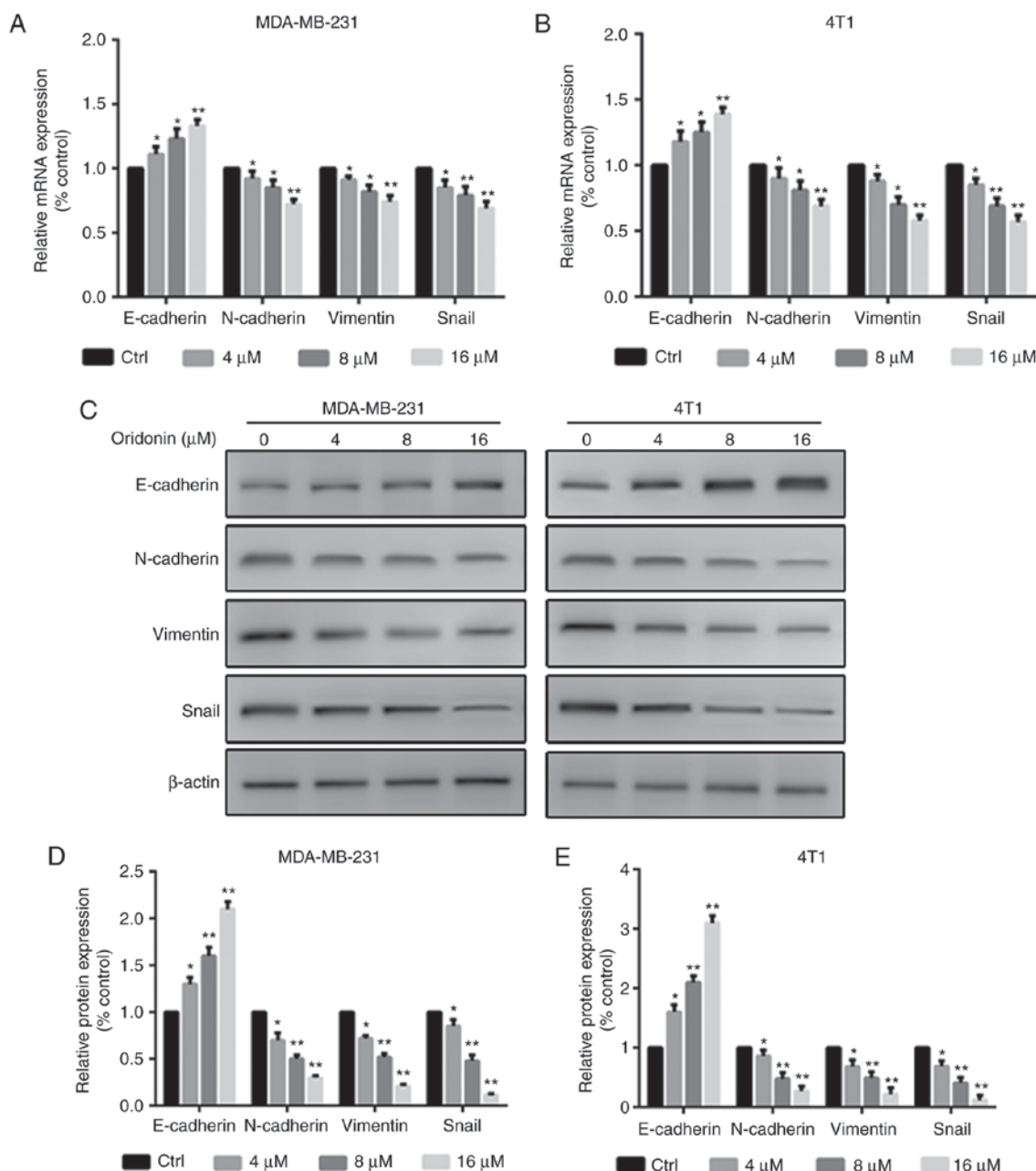


Figure 3. Effects of oridonin on EMT-associated marker mRNA and protein expression. (A) MDA-MB-231 and (B) 4T1 cells were pre-treated with indicated concentrations of oridonin for 24 h, followed by a reverse transcription-quantitative polymerase chain reaction assay to measure the regulatory effect of oridonin on mRNA expression of E-cadherin, N-cadherin, Vimentin and Snail. (C) MDA-MB-231 and 4T1 cells were pre-treated with indicated concentrations of oridonin for 24 h, followed by western blotting to examine the protein expression of E-cadherin, N-cadherin, Vimentin and Snail.  $\beta$ -actin was used as loading control. Relative protein expression for all proteins quantified using Image Pro Plus software in (D) MDA-MB-231 and (E) 4T1 cells. Data are presented as the mean  $\pm$  standard deviation of three independent experiments. \* $P < 0.05$  and \*\* $P < 0.01$  compared with the control group. Ctrl, control.

was performed. As presented in Fig. 2F and G, the capillary tube formation of HUVECs was significantly inhibited after 24 h exposure to oridonin when compared with the control group.

*Oridonin regulates the expression of EMT markers in MDA-MB-231 and 4T1 cells.* The results demonstrated that the effects of oridonin were dose-dependent, with significantly increasing expression levels of E-cadherin, and significantly decreasing expression levels of N-cadherin, Vimentin and Snail in MDA-MB-231 and 4T1 cells compared with the control group (Fig. 3).

*Oridonin suppresses the HIF-1 $\alpha$ /VEGF signaling pathway in MDA-MB-231 and 4T1 cells.* The expression levels of angiogenic molecules, including HIF-1 $\alpha$ , VEGF-A and VEGFR-2 were measured in MDA-MB-231 and 4T1 cells using western blotting. The data revealed that the levels of HIF-1 $\alpha$ , VEGF-A and VEGFR-2 were significantly reduced following oridonin treatment (Fig. 4A-C).

*Oridonin inhibits the tumor growth and angiogenesis in vivo.* To assess the effect of oridonin on tumor growth and angiogenesis *in vivo*, BALB/c mice were implanted with 4T1 cells. Following the injection of 4T1 cells, the tumors were allowed

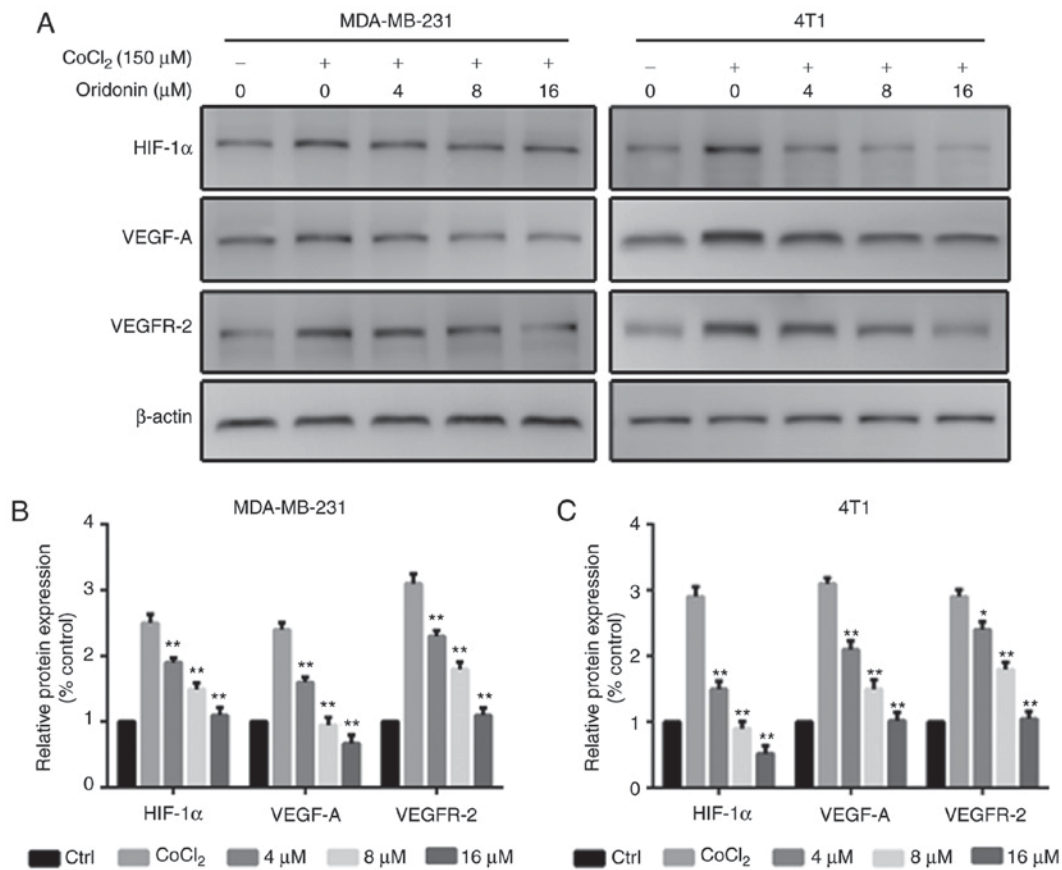


Figure 4. Effects of oridonin on HIF-1 $\alpha$ /VEGF signaling pathway protein expression. (A) MDA-MB-231 and 4T1 cells were pre-treated with indicated concentrations of oridonin for 24 h, followed by western blotting assay to test the protein expression of HIF-1 $\alpha$ , VEGF-A, VEGFR-2.  $\beta$ -actin was used as loading control. Relative protein expression for all proteins quantified using Image Pro Plus software in (B) MDA-MB-231 and (C) 4T1 cells. Data are presented as the mean  $\pm$  standard deviation of three independent experiments. \* $P < 0.05$  and \*\* $P < 0.01$  compared with the control group. Ctrl, control; VEGFR-A, vascular endothelium growth factor-A; VEGFR-2, vascular endothelium growth factor receptor-2.

to grow, subsequently mice were treated with different concentrations of oridonin. During the experiment, no mice presented multiple tumors. The longest diameter exhibited by a single subcutaneous tumor was  $\sim 6$  mm. No significant changes in the body weight of mice were noted followed oridonin treatment (Fig. 5A). The mean tumor volume after 9 days of treatment was significantly decreased in the group treated with indicated concentrations (2.5, 5 and 10 mg/kg) of oridonin (Fig. 5B). After 9 days of treatment, the mice were sacrificed; and the tumors were excised and weighted. The mean tumor weight after 9 days treatment was significantly decreased in all three oridonin treatment groups compared with the vehicle control (Fig. 5C). Additionally, the data demonstrated that oridonin significantly downregulated CD31 expression when compared with the control group (Fig. 5D and E). However, a limitation of the present study was absence of the determination of CD31 expression in the tissues by western blotting.

## Discussion

Recently, oridonin has attracted increasing attention due to its excellent antitumor activity against various cancer types, including breast cancer (20). The present study was designed to investigate the anti-metastatic effect of oridonin on breast cancer. The results of the present study demonstrated that oridonin significantly suppressed the migratory and invasive

potential of MDA-MB-231 and 4T1 cells *in vitro* possibly by inhibition of EMT and angiogenesis via downregulation of the HIF-1 $\alpha$ /VEGF signaling pathway.

As numerous literatures have reported, oridonin effectively inhibited the proliferation of a variety of cancer cells, including those from prostate (LNCaP, DU145, PC3), breast (MCF-7, MDA-MB231) and non-small cell lung (NCI-H520, NCI-H460, NCI-H1299) cancer, and acute promyelocytic leukemia (NB4) and glioblastoma multiforme (U118, U138) with the ED<sub>50</sub> range between 1.8 and 7.5 mg/ml (21). The majority of reported researches have investigated the cytotoxicity of oridonin. However, in the current study, the anti-metastatic ability of breast cancer cells below the cytotoxicity dosage was focused upon. Firstly, an MTT assay was performed to evaluate the inhibitory effects of oridonin on the proliferation of MDA-MB-231 and 4T1 cells. Oridonin significantly inhibited the proliferation of MDA-MB-231 and 4T1 cells in a dose-dependent manner. In order to eliminate the influence of cytotoxic effects of oridonin on the migratory and invasive capacities of cells, non-cytotoxic concentrations of 4, 8 and 16  $\mu$ M oridonin were chosen for further investigation. Cell invasion, migration and adhesion assays were performed to evaluate the anti-migratory ability of oridonin. Based on our previous study (22), the time of cell exposure to oridonin in the aforementioned experiments were as follows: Transwell invasion assay 24 h; wound healing migration assay

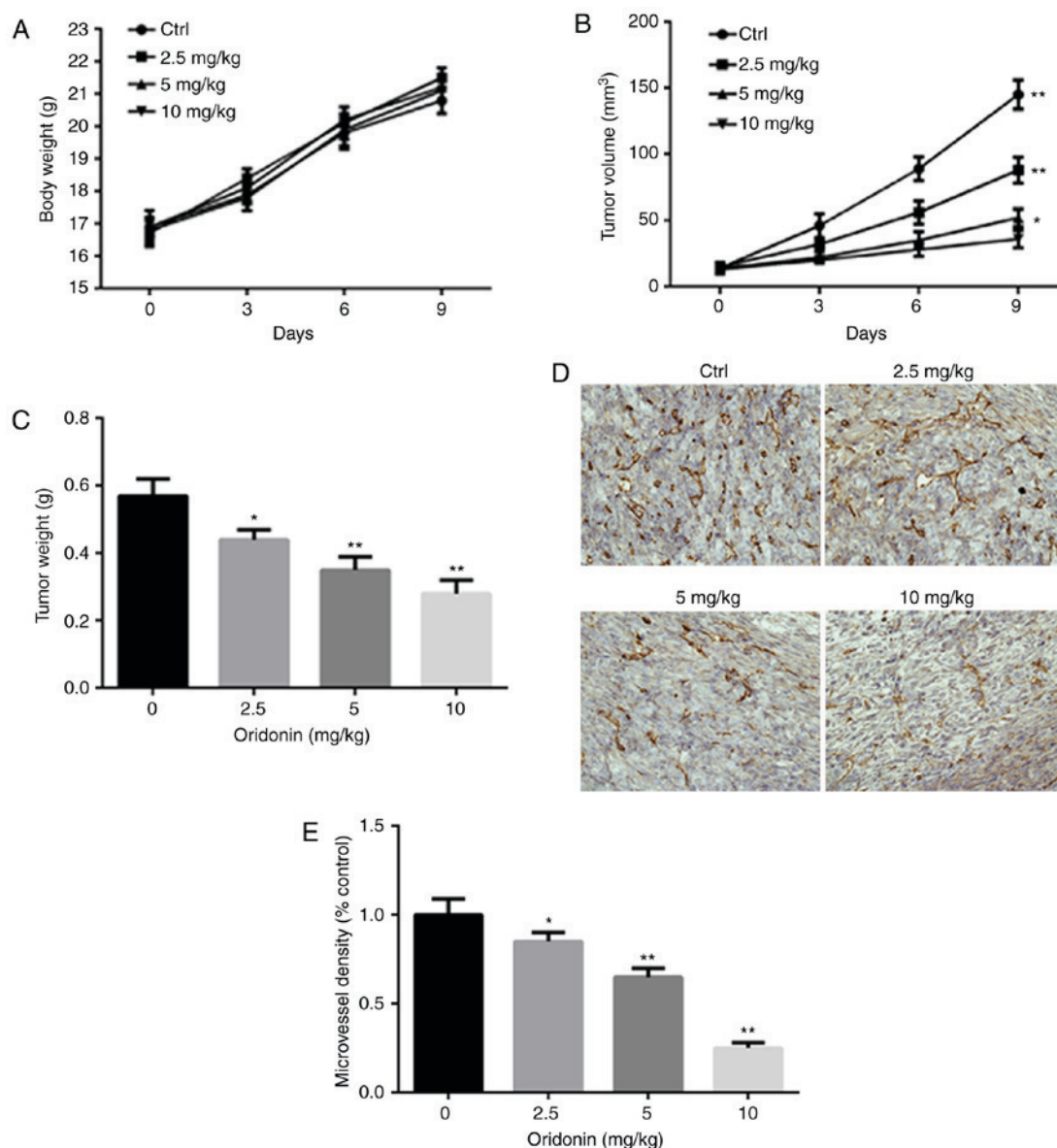


Figure 5. Effects of oridonin on the growth of xenografted 4T1 cells and angiogenesis *in vivo*. (A) Body weight and (B) tumor volume grow following treatment with oridonin. The treatment for each group was administered with indicated dosage every 3 days for four times/day. (C) Tumor weight at 9 days after treatment. (D) The vessels in tumor tissues were identified by immunohistochemical staining with antibodies against CD31 and (E) the microvessel density was quantified. CD31 was dyed as brown. Microvessel counts were performed at high power field (magnification, x200). Data are presented as the mean  $\pm$  standard deviation of six independent experiments. \* $P < 0.05$  and \*\* $P < 0.01$  compared with the control group. Ctrl, control; CD31, cluster of differentiation 31.

24 h; and cell adhesion assay 24 h. Hence, an exposure time of 48 h was chosen for the MTT assay, to demonstrate that the cytotoxicity of oridonin did not affect the migratory ability of tumor cells. The non-cytotoxic effects of 4, 8 and 16  $\mu\text{M}$  doses of oridonin were confirmed in non-tumorigenic human breast cells MCF-10A. No evident cytotoxic effects following exposure to oridonin for 48 h were observed in the MCF-10A cells. One limitation of the MTT assay was the absence of a time-dependent experiment on the effects of oridonin on cell viability, this may be investigated in further studies.

To the best of our knowledge, the results of the present study are the first to investigate the anti-migratory and invasive ability of oridonin on breast cancer cells below the cytotoxicity dosage. The metastasis potential of cancer cells is primarily determined by the migratory, invasive and adhesive capacities, which is commonly determined with wounding

healing, Transwell chamber with Matrigel-coated filter and adhesion assays, all three of which were used in the present study (23). The data demonstrated that oridonin effectively attenuated the migratory, invasive and adhesive abilities of MDA-MB-231 and 4T1 cells. In addition, to investigate the effect of oridonin on angiogenesis *in vitro*, a capillary tube formation assay was performed on HUVECs using Matrigel. It was observed that oridonin significantly inhibited capillary tube formation of HUVECs.

EMT is an essential step that occurs during cancer development. The initiation of EMT arises from a loss of cell polarity and cell-cell adhesion, which enhances the cancer cells migratory and invasive abilities. In breast cancer, EMT may be induced by multiple extracellular signaling factors, including tumor growth factor- $\beta$ , Notch, phosphatidylinositol 3-kinase/protein kinase B, Wnt and receptor tyrosine



kinases (24,25). The snail transcriptional repressor complex promotes EMT by repressing the junction component E-cadherin (26). Decreased E-cadherin has been associated with cancer cell migration, invasion and the advanced cancer stages, as well as metastasis, leading to poor prognosis in breast cancer (27). The results of the present study demonstrated that the expression of E-cadherin was significantly increased, and the expression of Snail, N-cadherin and Vimentin was significantly decreased following exposure to oridonin, indicating that the inhibition of EMT is involved in the anti-migratory and anti-invasive effects of oridonin.

Breast cancer shares the characteristics of tissue hypoxia, particularly when the tumor grows too quickly and angiogenesis fails to catch up with the speed of tumor growth. HIF-1 $\alpha$  is a key regulatory molecule that responds to hypoxia in cell migration, invasion, adhesion and angiogenesis (28). In addition, VEGF is associated with the induction of neovascularization in human breast cancer, which is mediated by multiple interacting genetic and environmental signals (29). A hypoxic microenvironment maybe a leading cause of angiogenesis, which is an important determinant of malignant tumor development, by activation of the expression of VEGF via HIF-1 $\alpha$  (30). In the *in vitro* study, it was revealed that oridonin exhibited an anti-angiogenesis effect. It is well known that angiogenesis is important for tumor metastasis. Thus, we hypothesized that the mechanism underlying the anti-migratory and anti-invasive effects of oridonin is associated with its anti-angiogenesis effect. Thus, an *in vivo* study was performed to confirm this hypothesis. As previously reported (31), the subcutaneously xenograft model is a better model to evaluate the effect of adrug or compound on angiogenesis using CD31 staining. Thus, this model was chosen in the present study. A metastatic mouse model will be established to evaluate the anti-metastatic effect of oridonin in future studies. The current study demonstrated that oridonin effectively inhibited tumor growth and angiogenesis *in vivo*. Further investigations revealed that the expression of HIF-1 $\alpha$ , VEGF-A and VEGFR-2 was significantly decreased, indicating that the inhibition of angiogenesis was involved in the antitumor effect of oridonin. Loss-of-function and gain-of-function experiments will be performed to confirm the mechanism underlying the antitumor effects of oridonin in further studies.

In conclusion, the findings of the present study suggest that oridonin significantly inhibited the migration, invasion, adhesion and angiogenesis through inhibition of EMT and downregulation of the HIF-1 $\alpha$ /VEGF signal pathway *in vitro* and *in vivo*. Thus, oridonin may be a potentially useful anti-metastatic agent in breast cancer treatment.

### Acknowledgements

The authors would like to thank Mr David Adam Jin from the International Medical School, Tianjin Medical School, China, for revising the manuscript.

### Funding

The present study was supported by the Natural Science Foundation of Tianjin Medical University (grant no. 2015KYZQ13), Postdoctoral Science Foundation of China

(grant no. 2016M591398) and Basic Scientific Research Fund of Tianjin Municipal Education Commission (grant no. 2016YD07).

### Availability of data and materials

The datasets used or analyzed during the current study are available from the corresponding author on reasonable request.

### Authors' contributions

CL and QW conceived and designed the experiments. CL, QW, SS and XW performed the experiments. CL and GL analyzed the data. CL and QW contributed reagents/materials/analysis tools and wrote the manuscript.

### Ethics approval and consent to participate

All animal experiments were approved by the Animal Ethics Committee of Tianjin Medical University and complied with its regulations.

### Patient consent for publication

Not applicable.

### Competing interests

The authors declare that they have no competing interests.

### References

- Ramasamy T, Sundaramoorthy P, Ruttala HB, Choi Y, Shin WH, Jeong JH, Ku SK, Choi HG, Kim HM, Yong CS and Kim JO: Polyunsaturated fatty acid-based targeted nanotherapeutics to enhance the therapeutic efficacy of docetaxel. *Drug Deliv* 24: 1262-1272, 2017.
- Neelakantan D, Zhou H, Oliphant MUJ, Zhang X, Simon LM, Henke DM, Shaw CA, Wu MF, Hilsenbeck SG, White LD, *et al*: EMT cells increase breast cancer metastasis via paracrine GLI activation in neighbouring tumour cells. *Nat Commun* 8: 15773, 2017.
- Zhou T, Zhang A, Kuang G, Gong X, Jiang R, Lin D, Li J, Li H, Zhang X, Wan J and Li H: Baicalin inhibits the metastasis of highly aggressive breast cancer cells by reversing epithelial-to-mesenchymal transition by targeting  $\beta$ -catenin signaling. *Oncol Rep* 38: 3599-3607, 2017.
- Sohn EJ, Jung DB, Lee H, Han I, Lee J, Lee H and Kim SH: CNOT2 promotes proliferation and angiogenesis via VEGF signaling in MDA-MB-231 breast cancer cells. *Cancer Lett* 412: 88-98, 2018.
- Zhang Y, Liu J, Lin J, Zhou L, Song Y, Wei B, Luo X, Chen Z, Chen Y, Xiong J, *et al*: The transcription factor GATA1 and the histone methyltransferase SET7 interact to promote VEGF-mediated angiogenesis and tumor growth and predict clinical outcome of breast cancer. *Oncotarget* 7: 9859-9875, 2016.
- Yehia L, Boulos F, Jabbour M, Mahfoud Z, Fakhruddin N and El-Sabban M: Expression of HIF-1 $\alpha$  and markers of angiogenesis are not significantly different in triple negative breast cancer compared to other breast cancer molecular subtypes: Implications for future therapy. *PLoS One* 10: e0129356, 2015.
- Pakravan K, Babashah S, Sadeghizadeh M, Mowla SJ, Mossahebi-Mohammadi M, Ataei F, Dana N and Javan M: MicroRNA-100 shuttled by mesenchymal stem cell-derived exosomes suppresses *in vitro* angiogenesis through modulating the mTOR/HIF-1 $\alpha$ /VEGF signaling axis in breast cancer cells. *Cell Oncol* 40: 457-470, 2017.

8. Shao C, Zhang J, Fu J and Ling F: The potential role of Brachyury in inducing epithelial-to-mesenchymal transition (EMT) and HIF-1 $\alpha$  expression in breast cancer cells. *Biochem Biophys Res Commun* 467: 1083-1089, 2015.
9. He Z, Xiao X, Li S, Guo Y, Huang Q, Shi X, Wang X and Liu Y: Oridonin induces apoptosis and reverses drug resistance in cisplatin resistant human gastric cancer cells. *Oncol Lett* 14: 2499-2504, 2017.
10. Dong Y, Zhang T, Li J, Deng H, Song Y, Zhai D, Peng Y, Lu X, Liu M, Zhao Y and Yi Z: Oridonin inhibits tumor growth and metastasis through anti-angiogenesis by blocking the Notch signaling. *PLoS One* 9: e113830, 2014.
11. Liu H, Qian C and Shen Z: Anti-tumor activity of oridonin on SNU-5 subcutaneous xenograft model via regulation of c-Met pathway. *Tumour Biol* 35: 9139-9146, 2014.
12. Cui XY, Tinholt M, Stavik B, Dahm AE, Kanse S, Jin Y, Seidl S, Sahlberg KK, Iversen N, Skretting G and Sandset PM: Effect of hypoxia on tissue factor pathway inhibitor expression in breast cancer. *J Thromb Haemost* 14: 387-396, 2016.
13. Lopes FC, Ferreira R, Albuquerque DM, Silveira AA, Costa R, Soares R, Costa FF and Conran N: In vitro and in vivo anti-angiogenic effects of hydroxyurea. *Microvasc Res* 94: 106-113, 2014.
14. Chen H, Zhang L, Long X, Li P, Chen S, Kuang W and Guo J: Sargassum fusiforme polysaccharides inhibit VEGF-A-related angiogenesis and proliferation of lung cancer in vitro and in vivo. *Biomed Pharmacother* 85: 22-27, 2017.
15. Kang Z, Jiang W, Luan H, Zhao F and Zhang S: Cornin induces angiogenesis through PI3K-Akt-eNOS-VEGF signaling pathway. *Food Chem Toxicol* 58: 340-346, 2013.
16. Livak KJ and Schmittgen TD: Analysis of relative gene expression data using real-time quantitative PCR and the 2(-Delta Delta C(T)) method. *Methods* 25: 402-408, 2001.
17. An J, Wang L, Zhao Y, Hao Q, Zhang Y, Zhang J, Yang C, Liu L, Wang W, Fang D, *et al*: Effects of FSTL1 on cell proliferation in breast cancer cell line MDA-MB-231 and its brain metastatic variant MDA-MB-231-BR. *Oncol Rep* 38: 3001-3010, 2017.
18. Hu H, Huang G, Wang H, Li X, Wang X, Feng Y, Tan B and Chen T: Inhibition effect of triptolide on human epithelial ovarian cancer via adjusting cellular immunity and angiogenesis. *Oncol Rep* 39: 1191-1196, 2017.
19. Ko P, Kim D, You E, Jung J, Oh S, Kim J, Lee KH and Rhee S: Extracellular matrix rigidity-dependent sphingosine-1-phosphate secretion regulates metastatic cancer cell invasion and adhesion. *Sci Rep* 6: 21564, 2016.
20. Xia S, Zhang X, Li C and Guan H: Oridonin inhibits breast cancer growth and metastasis through blocking the Notch signaling. *Saudi Pharm J* 25: 638-643, 2017.
21. Ikezoe T, Chen SS, Tong XJ, Heber D, Taguchi H and Koeffler HP: Oridonin induces growth inhibition and apoptosis of a variety of human cancer cells. *Int J Oncol* 23: 1187-1193, 2003.
22. Li CY, Wang Q, Shen S, Wei XL and Li GX: Oridonin inhibits migration, invasion, adhesion and TGF- $\beta$ 1-induced epithelial-mesenchymal transition of melanoma cells by inhibiting the activity of PI3K/Akt/GSK-3 $\beta$  signaling pathway. *Oncol Lett* 15: 1362-1372, 2018.
23. Li Y and Galileo DS: Soluble L1CAM promotes breast cancer cell adhesion and migration in vitro, but not invasion. *Cancer Cell Int* 10: 34, 2010.
24. Matysiak M, Kapka-Skrzypczak L, Jodłowska-Jędrych B and Kruszewski M: EMT promoting transcription factors as prognostic markers in human breast cancer. *Arch Gynecol Obstet* 295: 817-825, 2017.
25. Yan LX, Liu YH, Xiang JW, Wu QN, Xu LB, Luo XL, Zhu XL, Liu C, Xu FP, Luo DL, *et al*: PIK3R1 targeting by miR-21 suppresses tumor cell migration and invasion by reducing PI3K/AKT signaling and reversing EMT, and predicts clinical outcome of breast cancer. *Int J Oncol* 48: 471-484, 2016.
26. Huang T, Chen Z and Fang L: Curcumin inhibits LPS-induced EMT through downregulation of NF- $\kappa$ B-Snail signaling in breast cancer cells. *Oncol Rep* 29: 117-124, 2013.
27. Yu JM, Sun W, Hua F, Xie J, Lin H, Zhou DD and Hu ZW: BCL6 induces EMT by promoting the ZEB1-mediated transcription repression of E-cadherin in breast cancer cells. *Cancer Lett* 365: 190-200, 2015.
28. Kim DH, Sung B, Kim JA, Kang YJ, Hwang SY, Hwang NL, Suh H, Choi YH, Im E, Chung HY and Kim ND: HS-1793, a resveratrol analogue, downregulates the expression of hypoxia-induced HIF-1 and VEGF and inhibits tumor growth of human breast cancer cells in a nude mouse xenograft model. *Int J Oncol* 51: 715-723, 2017.
29. Zhang E, Shi H, Yang L, Wu X and Wang Z: Ginsenoside Rd regulates the Akt/mTOR/p70S6K signaling cascade and suppresses angiogenesis and breast tumor growth. *Oncol Rep* 38: 359-367, 2017.
30. Liang S, Chen Z, Jiang G, Zhou Y, Liu Q, Su Q, Wei W, Du J and Wang H: Activation of GPER suppresses migration and angiogenesis of triple negative breast cancer via inhibition of NF- $\kappa$ B/IL-6 signals. *Cancer Lett* 386: 12-23, 2017.
31. Cook MT, Liang Y, Besch-Williford C, Goyette S, Mafuvadze B and Hyder SM: Luteolin inhibits progesterin-dependent angiogenesis, stem cell-like characteristics, and growth of human breast cancer xenografts. *Springerplus* 4: 444, 2015.



This work is licensed under a Creative Commons Attribution-NonCommercial-NoDerivatives 4.0 International (CC BY-NC-ND 4.0) License.